Journal of Molecular Catalysis A: Chemical 345 (2011) 60–68

Contents lists available at ScienceDirect

Journal of Molecular Catalysis A: Chemical

journal homepage: www.elsevier.com/locate/molcata

The influence of La doping on the catalytic behavior of Cu/ZrO_2 for methanol synthesis from CO_2 hydrogenation

Xiaoming Guo[a,b], Dongsen Mao[a,*], Guanzhong Lu[a,b,**], Song Wang[a], Guisheng Wu[a]

[a] Research Institute of Applied Catalysis, School of Chemical and Environmental Engineering, Shanghai Institute of Technology, Shanghai 200235, PR China
[b] Research Institute of Industrial Catalysis, East China University of Science and Technology, Shanghai 200237, PR China

ARTICLE INFO

Article history:
Received 18 January 2011
Received in revised form 4 May 2011
Accepted 22 May 2011
Available online 27 May 2011

Keywords:
Cu/ZrO_2 catalyst
La doping
Methanol synthesis
CO_2 hydrogenation
Activity and selectivity

ABSTRACT

A series of Cu/ZrO_2 catalysts with various La loadings for methanol synthesis from CO_2 hydrogenation were prepared by a urea–nitrate combustion method. The catalysts were characterized with N_2 adsorption, XRD, reactive N_2O adsorption, XPS, TPR, H_2-TPD and CO_2-TPD techniques, and tested for methanol synthesis from CO_2 hydrogenation. With increasing La loading, the Cu surface area increases first and then decreases, whereas the amount of basic site over catalysts increases continuously. The results of catalytic test reveal that a linear relationship exists between the conversion of CO_2 and the Cu surface area. Moreover, it is found for the first time that the selectivity to methanol is related to the distribution of basic site on the catalyst surface. The presence of La favors the production of methanol, and the optimum catalytic activity is obtained when the amount of La doping is 5% of the total amount of Cu^{2+} and Zr^{4+}.

1. Introduction

With the increase in CO_2 concentration in the atmosphere, the global warming problems are becoming more and more serious. Conversion of CO_2 to useful chemicals and fuels may be one of the promising ways to mitigate the problem. Most of the existing research focuses on CO_2 hydrogenation to methanol because methanol is an important feedstock for the organic chemical industry and a potential alternative to fossil fuels [1,2]. Based on the great significance of methanol synthesis from CO_2 hydrogenation, a new concept of "methanol economy" was proposed by Olah et al. [1].

It has been widely reported that the Cu catalysts supported on zirconia exhibit high catalytic activity for methanol synthesis from CO_2 hydrogenation [3–11]. A number of novel preparation methods have been developed to prepare Cu/ZrO_2-based catalysts [3–9]. Furthermore, the effects of synthesis conditions, pre-treatment process, and precursors on the structures and properties of the catalysts were investigated [6–8,10,11]. Apart from the preparation methods and preparation conditions, the influence of promoter on the performance of Cu/ZrO_2-based were also explored [5,12–15]. For example, Kilo et al. [12] studied the effects of chromium- and manganese oxide on the structural and catalytic properties of Cu/ZrO_2. They found that the presence of Mn or Cr suppressed sintering of the copper crystallites and stabilized the amorphous state of zirconia, which resulted in an increased thermal stability of the catalyst. Liu et al. [5] prepared the B_2O_3 and Ga_2O_3 promoted Cu/ZrO_2 catalysts using nanocrystalline zirconia as the support, and revealed that the introduction of B and Ga changed the content of surface CuO. Moreover, a series of Cu/ZrO_2-based catalysts promoted by oxides of B, Mn, In, Gd, Y, Mg and Ga were reported by Słoczyński et al. [13,14]. They found that the promoters influenced the dispersion of Cu, the surface composition of the catalyst and the catalytic activity in the reaction of methanol synthesis. The highest yield of methanol was observed for the catalyst with the Ga_2O_3 additive.

To better understand and design the highly active catalysts for methanol synthesis from CO_2 hydrogenation, some research concerning the reaction mechanism has been carried out. Bianchi et al. [16] reported that there existed the spillover of adsorbed hydrogen in the interface of zirconia and copper. Bell and co-workers [17–21] studied the reaction mechanism for methanol synthesis from CO and CO_2 over Cu/ZrO_2-based catalysts, and proposed a dual-site or bifunctional mechanism. Recently, Arena et al. [22] investigated the reaction of CO_2 hydrogenation on $Cu–ZnO/ZrO_2$, and similar viewpoint was presented. According to the dual-site or bifunctional mechanism, the adsorption and dissociation of hydrogen occur over the Cu site, while the adsorption of CO_2 takes place on the ZrO_2 site. Then, the atomic hydrogen transports from the surface of Cu onto the surface of ZrO_2 via spillover and hydrogenates the adsorbed

* Corresponding author. Tel.: +86 21 6494 1386; fax: +86 21 6494 1386.
** Corresponding author at: Research Institute of Applied Catalysis, School of Chemical and Environmental Engineering, Shanghai Institute of Technology, Shanghai 200235, PR China. Tel.: +86 21 6087 3300; fax: +86 21 6087 3300.
E-mail addresses: dsmao1106@yahoo.com.cn (D. Mao), gzhlu@ecust.edu.cn (G. Lu).

1381-1169/$ – see front matter © 2011 Elsevier B.V. All rights reserved.
doi:10.1016/j.molcata.2011.05.019

carbon containing species to methanol. On this account, it is reasonable to draw a conclusion that a high surface area of Cu and appropriate adsorption amount and adsorption strength of CO_2 are favorable for the hydrogenation of CO_2. This gives a guideline for the design of high effective catalysts for methanol synthesis from hydrogenation of CO_2. La_2O_3, a rare earth sesquioxide, is frequently used as catalyst promoter for its sintering-resistant property [23]. In addition, La_2O_3 exhibits high basicity, and it is an interesting candidate as active phase in processes catalyzed by solid base [24,25]. It could be expected that the introduction of La_2O_3 into Cu/ZrO_2 catalyst will affect the dispersion of Cu and the surface basicity of catalyst, which in turn affects the adsorption of H_2 and CO_2, respectively.

The objective of this work is to explore the effect of La doping on the properties of Cu/ZrO_2 catalysts. The physicochemical properties of La-promoted catalysts were characterized by XRD, BET, reactive N_2O adsorption, XPS, TPR, H_2-TPD and CO_2-TPD techniques, and the catalytic activity for methanol synthesis from CO_2 hydrogenation was evaluated. To gain more insight into the mechanism for the methanol synthesis, the relation between the physicochemical properties, especially the metallic copper surface area and the CO_2 adsorption behavior over the catalysts, and the catalytic behavior were discussed in detail.

2. Experimental

2.1. Catalyst preparation

Cu/ZrO_2 catalysts with various La loadings were prepared by the urea–nitrate combustion method. All chemicals used in this work were of reagent grade purity (Shanghai Chemical Reagent Corporation, PR China). Firstly, the required amounts of metal nitrates were dissolved in deionized water to form a solution, in which the Cu^{2+}/Zr^{4+} molar ratio maintained to be 1:1, while the molar percentage of La^{3+} ranged from 1% to 10% relative to the total amount of Cu^{2+} and Zr^{4+}. Then 0.1 mol/L solution of urea was slowly added to the metal nitrate solution under constant stirring. The resulting mixture was kept in an ultrasound bath operating at 47 kHz with a power of 30 W for 0.5 h until a white slurry was obtained. Afterward, the slurry was transferred to an open muffle furnace preheated at 573 K. The slurry started boiling with frothing and foaming, and ignited spontaneously in a couple of minutes with rapid evolution of a large quantity of gases, yielding a foamy, voluminous powder. Because the time for the autoignition was rather short, to remove traces of undecomposed urea, nitrates, and their decomposition products, the powder was further heated at 773 K for 4 h. To obtain an optimum catalytic performance, the amount of urea used in the combustion process was 50% of the stoichiometric amount, which can be calculated according to propellant chemistry [26]. A more detailed description of the preparation process was given in Ref. [8]. La_2O_3, used as the La reference in this study, was prepared via the thermal decomposition of $La(NO_3)_3$ at 973 K. In this paper, the undoped Cu/ZrO_2 catalyst is denoted as CZ, and the La doped Cu/ZrO_2 catalysts are denominated as *x*%LCZ, where "*x*%" is the molar percentage of La^{3+} relative to the total amount of Cu^{2+} and Zr^{4+}.

2.2. Catalyst characterization

X-ray diffraction (XRD) patterns were recorded with a PANalytical X'Pert diffractometer operating with Ni β-filtered Cu Kα radiation at 40 kV and 40 mA. Two theta angles ranged from 10° to 70° with a speed of 6° per minute.

Full nitrogen adsorption/desorption isotherms at 77 K were obtained after outgassing the sample under vacuum at 473 K for 4 h, using a Micromeritics ASAP2020 M+C adsorption apparatus. The BET specific surface area (S_{BET}) was calculated using a value of 0.162 nm^2 for the cross-sectional area of the nitrogen molecule.

The metallic copper surface area (S_{Cu}) in the reduced catalyst was determined using a N_2O chemisorption method similar to that described by Chinchen et al. [27]. Once the catalyst was reduced in an H_2/He mixture at 523 K for 1 h, it was exposed to a flow of He and cooled to the chemisorption temperature (333 K). Then, a flow of 1 vol% N_2O/He gas mixture was fed into the reactor. The N_2 produced by the decomposition of N_2O on the exposed Cu atoms was detected using a mass spectrometer (Pfeiffer Vacuum Quadstar, 32-bit). The metallic copper surface area was calculated assuming an atomic copper surface density of 1.46×10^{19} Cu atoms/m^2 and a molar stoichiometry of $N_2O/Cu = 0.5$ [22].

X-ray photoelectron spectroscopy (XPS) measurements were performed on a Kratos Axis Ultra DLD spectrometer equipped with a Al Kα (1486.6 eV) X-ray exciting source. The pass energy of the analyser was set at 40 eV. The binding energies were referenced to the adventitious C 1s peak at 284.6 eV (accuracy within ±0.1 eV).

Temperature-programmed reduction (TPR) measurements were performed in a continuous-flow apparatus fed with a 10% H_2/N_2 mixture flowing at 50 ml/min and heated at a rate of 5 K/min. A ca. 30-mg catalyst sample was used, with H_2 consumption monitored by a thermal conductivity detector (TCD).

Hydrogen temperature programmed desorption (H_2-TPD) was carried out in a quartz tubular reactor. Firstly, the catalyst sample was reduced at 573 K for 1 h in a flowing of 10% H_2/N_2 mixture. Then the sample was cooled to room temperature and further saturated in H_2/N_2 mixture for 1 h, followed by flushing in N_2 for 1 h. The TPD measurements were conducted in a N_2 stream (50 ml/min) from room temperature to 773 K at a heating rate of 5 K/min. The change of hydrogen signal was monitored by a TCD and quantitatively calibrated by H_2 pulses.

The basicity of the catalyst was measured by CO_2 temperature-programmed desorption (CO_2-TPD). Prior to the adsorption of CO_2, the catalysts were heated at 773 K for 60 min for cleaning the surface from moisture and other adsorbed gases. After cooling to room temperature, the catalyst was saturated with pure CO_2 (25 ml/min) at 323 K for 60 min, and then flushed with He flow (50 ml/min) to remove any physisorbed molecules. Afterward, the TPD experiment was started with a heating rate of 5 K/min under He flow (50 ml/min), and the desorbed CO_2 was detected by a mass spectrometer (Pfeiffer Vacuum Quadstar, 32-bit). The amount of the desorbed CO_2 was quantified by comparing the integrated area of the TPD curves to the peak area of the injected CO_2 calibration pulse.

2.3. Catalyst testing

Activity and selectivity measurements for CO_2 hydrogenation were carried out in a continuous-flow, fixed-bed reactor. About 0.5 g of catalyst diluted with quartz sand (both in 20–40 mesh) was packed into the stainless steel tubular reactor (5 mm i.d.). Preliminary experiments with respect to possible influence caused by interparticle mass transfer limitation confirmed that such limitation could be ruled out under the conditions used in the present study. Prior to the catalytic measurements, the fresh catalyst was reduced in a stream of 10% H_2/N_2 flowing at 30 ml/min at 573 K for 3 h under atmospheric pressure. Then the reactor was cooled to a given temperature and a gas mixture (CO_2:H_2:N_2 = 22:66:12, molar) was introduced, raising the pressure to 3.0 MPa. All post-reactor lines and valves were heated to 413 K to prevent product condensation. Effluent products were analyzed on-line with a gas chromatograph (6820, Agilent). Methanol was determined with a Porapak Q column, a FID detector and Carbosieve column, TCD detector for other gaseous products were used. Conversion and selectivity values were calculated by mass-balance method and the

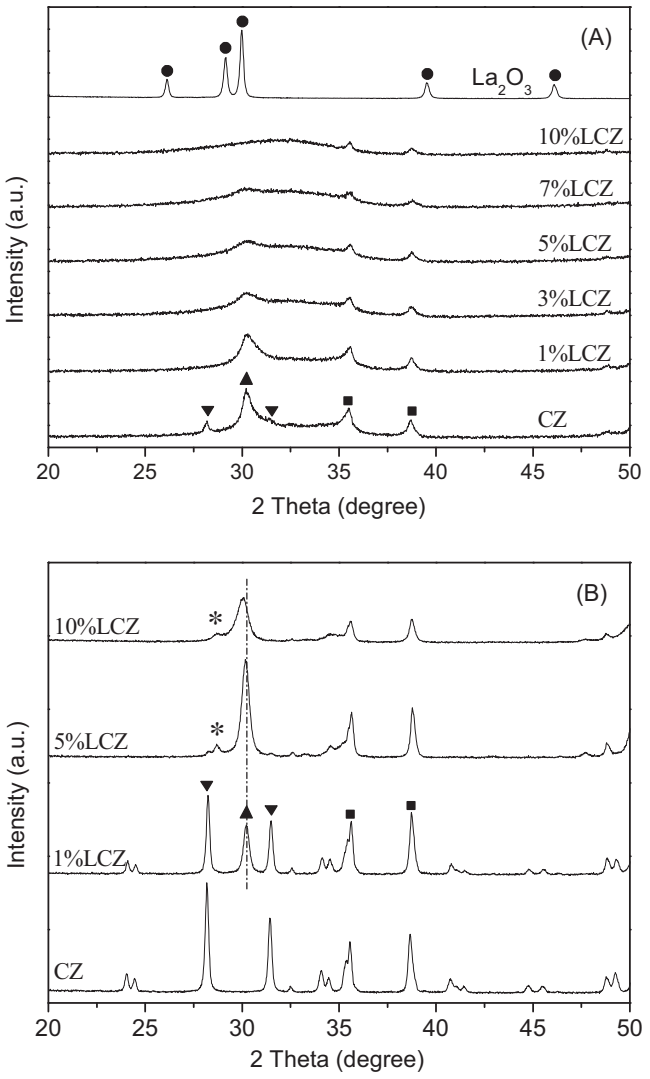

Fig. 1. XRD patterns of Cu/ZrO_2 catalysts with different La loadings: (A) calcined at 773 K and (B) calcined at 1073 K. (■) CuO; (▲) ZrO_2 (tetragonal); (▼) ZrO_2 (monoclinic); (●) La_2O_3; (*) $La_2Zr_2O_7$.

steady-state values were quoted as the average of four different analyses taken after 5 h on stream operation.

3. Results

3.1. The textural and structural properties

The XRD patterns of Cu/ZrO_2 catalysts with various La loadings calcined at 773 K are shown in Fig. 1(A). For comparison, the X-ray diffractogram of pure lanthana is also presented. The diffraction peaks at 2θ of 35.6° and 38.8° were ascribed to CuO phase (JCPDS 80-1268). With the increase in the content of La dopant, the intensity of diffraction peak for CuO weakened gradually, while the peak width broadened slightly. This indicates that the crystallization degree of CuO, as well as the particle sizes of CuO crystallites though it cannot be determined accurately with the Scherrer equation since the CuO XRD reflection is weak, decrease with increasing the La loading. The characteristic X-ray diffraction peaks for tetragonal zirconia (t-ZrO_2, 2θ = 30.3°, JCPDS 88-1007) and monoclinic ZrO_2 (m-ZrO_2, 2θ = 28.2°, 31.5°, JCPDS 83-0940) can be detected on the undoped Cu/ZrO_2 sample. With the introduction of La, the diffraction peaks of t-ZrO_2 become weak and broad, and the diffraction peaks of m-ZrO_2 disappear completely. When the content of La dopant exceeds 5%, the zirconia exists mainly in amorphous form. Similar results were reported by Chuah et al. [28], who found that the doping of La was unfavorable for the crystallization of ZrO_2 and the growth of ZrO_2 crystallite. As shown in Fig. 1(A), no diffraction peaks of La_2O_3 crystallites can be found for all the studied samples, suggesting the formation of finely dispersed La_2O_3 on the surface of catalyst, or the formation of La_2O_3–ZrO_2 non-crystalline compound, which could not be detected by XRD technique due to the low degree of crystallization [29].

Table 1
Physicochemical properties and apparent activation energy of the Cu/ZrO_2 catalysts with different La loadings.

Catalysts	S_{BET} (m^2/g)	S_{Cu} (m^2/g)	$E_a(CH_3OH)$ (kJ/mol)	$E_a(CO)$ (kJ/mol)
CZ	36	2.83	40	87
1%LCZ	40	3.22	39	99
3%LCZ	52	3.74	–	–
5%LCZ	54	4.36	38	102
7%LCZ	59	3.78	–	–
10%LCZ	58	3.55	38	108

To obtain further information about the structure of the catalysts, they were calcined at 1073 K for 4 h and examined by XRD. As shown in Fig. 1(B), for the undoped Cu/ZrO_2 sample, the diffraction peaks of t-ZrO_2 disappear, accompanied by the appearance of the high and sharp diffraction peaks of m-ZrO_2. This is attributed to the transformation from t-ZrO_2 to m-ZrO_2 as the temperature is higher than 923 K [30]. With the introduction of La, the diffraction peaks of t-ZrO_2 reappear. As the content of La loading reaches 5%, the diffraction peaks of m-ZrO_2 vanish. This phenomenon indicates that the phase transformation from t-ZrO_2 to m-ZrO_2 is suppressed by the incorporation of La [28]. It is noteworthy that a diffraction peak appears at 2θ of 28.7°, which is a characteristic diffraction peak of $La_2Zr_2O_7$ (JCPDS 71-2363). On the other hand, there is still no diffraction of La_2O_3 crystallites in the XRD pattern. On these accounts, it can address that La_2O_3 exists mainly in a form of $La_2Zr_2O_7$. Furthermore, the introduction of La leads to a slight shift of t-ZrO_2 diffraction peak to lower 2θ values, as shown in Fig. 1(B). This is indicative of an increase in the crystal lattice parameter, which is originated from the substitution of Zr^{4+} (radius 0.86 Å) by La^{3+} cations (radius 1.06 Å) [31].

The BET specific surface area (S_{BET}) is listed in Table 1. A marked increase in S_{BET} was observed from 36 m^2/g of CZ to 54 m^2/g of 5%LCZ. As the addition of La exceeded 5%, the S_{BET} increased slowly. This result is in accordance with the results regarding the crystallite size, as determined from XRD. The metallic copper surface area (S_{Cu}), which was determined by N_2O titration, is also presented in Table 1. It can be seen that the S_{Cu} increased first and then decreased with the increase in La loading. A maximum of 4.4 m^2/g was obtained over 5%LCZ.

3.2. XPS analysis

The binding energies (BE) of Cu $2p_{3/2}$ and Zr $3d_{5/2}$ core electrons are summarized in Table 2. All the catalysts exhibit Cu $2p_{3/2}$ main peaks at about 940.1 eV accompanied by intense shake-up peaks at about 942.0 eV, which means that the chemical state of copper is Cu^{2+}. There are no significant variations in the binding energies of copper with increasing La dopant concentration. However, the BE of Zr $3d_{5/2}$ shifts slightly from 181.8 to 181.5 eV as the La content increases from zero to 10%, demonstrating the existence of an interaction between ZrO_2 and La_2O_3.

Surface compositions of the catalysts determined with the XPS method are listed in Table 2. Compared with the nominal compositions, the surface of catalyst is considerably depleted of Cu. In contrast, an enrichment of Zr and La on the surface is observed. Similar results were obtained for the chromium- and manganese

Table 2
XPS results for Cu/ZrO_2 catalysts with different La loadings.

Catalyst	Binding energy (eV)		Relative surface concentration of metal[a] (at.%)			Cu/Zr molar ratio
	Cu $2p_{3/2}$	Zr $3d_{5/2}$	Cu	Zr	La	
CZ	934.1	181.8	32.5 (50.0)	67.5 (50.0)	–	0.48
1%LCZ	934.1	181.6	34.1 (49.5)	63.1 (49.5)	2.8 (1.0)	0.54
5%LCZ	934.0	181.5	32.7 (47.6)	59.5 (47.6)	7.8 (4.8)	0.55
10%LCZ	934.1	181.5	24.1 (45.5)	63.0 (45.5)	12.9 (9.0)	0.38

[a] Values in parenthesis are nominal fraction of metal.

Table 3
Temperatures of reduction peaks and their contributions to the TPR pattern over Cu/ZrO_2 catalysts with different La loadings.

Catalysts	T_α (K)	T_β (K)	$A_\alpha/(A_\alpha + A_\beta)$[a] (%)
CZ	448	493	7.3
1%LCZ	446	494	25.4
3%LCZ	444	487	29.6
5%LCZ	444	489	34.2
7%LCZ	441	487	27.5
10%LCZ	440	487	23.1

[a] A_α and A_β represent the areas of α and β peaks, respectively.

oxide promoted Cu/ZrO_2 catalysts [12]. Moreover, the Cu/Zr ratios are also included in Table 2. Clearly, the Cu/Zr ratios are much lower than the nominal ratio of Cu/Zr (Cu:Zr = 1:1), and a maximum of 0.55 is obtained as the content of La loading reached 5%.

3.3. H_2-TPR analysis

In order to assess the reduction behavior of the catalysts, TPR measurements were performed. Fig. 2 shows the H_2-TPR profiles of the studied samples. All of the samples exhibit two reduction peaks between 425 and 550 K. As well documented, the low temperature peak (α peak) is attributed to the reduction of highly dispersed CuO surface species, whereas the peak appearing at higher temperature (β peak) is related to the reduction of the bulk-like CuO [32,33]. Since the highly dispersed CuO species are considered to contribute mainly to catalytic activity [33], the relative contributions of α peak to the TPR pattern are summarized in Table 3. In addition, the peak positions are also listed in Table 3. It can be seen that, with the addition of La, the fractions of α peak increase from 7.3% of the La-free Cu/ZrO_2 to 34.2% of 5%LCZ. Further increase in La loading results in a decrease in the fractions of α peak. On the other hand, as shown in Table 3, the positions of α peak shift to lower temperatures with the increase in La loadings. Similar change of β peak position can also be observed although the variation trend is not as distinct as that of α peak. Moreover, it should be noted that the reduction of La_2O_3 and ZrO_2 is thermodynamically feasible, but they cannot be reduced within the experimental region [34,35].

3.4. H_2-TPD analysis

The H_2-TPD profiles on the pre-reduced catalysts are presented in Fig. 3. Two desorption peaks can be observed for all the investigated catalysts. The low temperature peaks (peak α) located in the range of 361–374 K represent the desorption of atomic hydrogen on the surface of metallic Cu [22]. The high temperature peaks (peak β) centered at 653 K are due to the desorption of strongly adsorbed hydrogen over ZrO_2 [36,37]. As reported in the literature [37], pure ZrO_2 hardly adsorbs any hydrogen, but ZrO_2 in Cu/ZrO_2 can serve as a reservoir of hydrogen because hydrogen can transport from Cu to ZrO_2 via spillover. The maximum desorption temperature and quantitative data are listed in Table 4. The amounts of H_2 desorbed from Cu sites take on a volcanic trend with increasing La loading, and a maximum is obtained over 5%LCZ. This is in good agreement with the variation trend of S_{Cu}. In addition, the amounts of H_2 desorbed from ZrO_2 sites are close to each other, which suggest that the introduction of La has no significant influence on the ability of hydrogen storage of Cu/ZrO_2 catalysts.

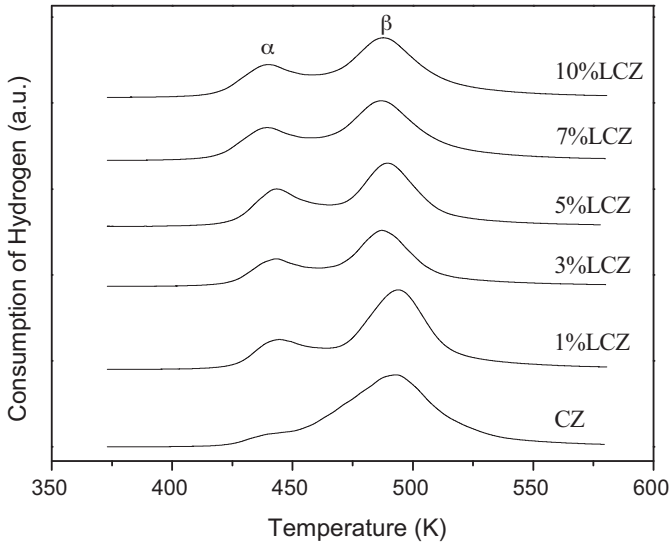

Fig. 2. H_2-TPR profiles of Cu/ZrO_2 catalysts with different La loadings.

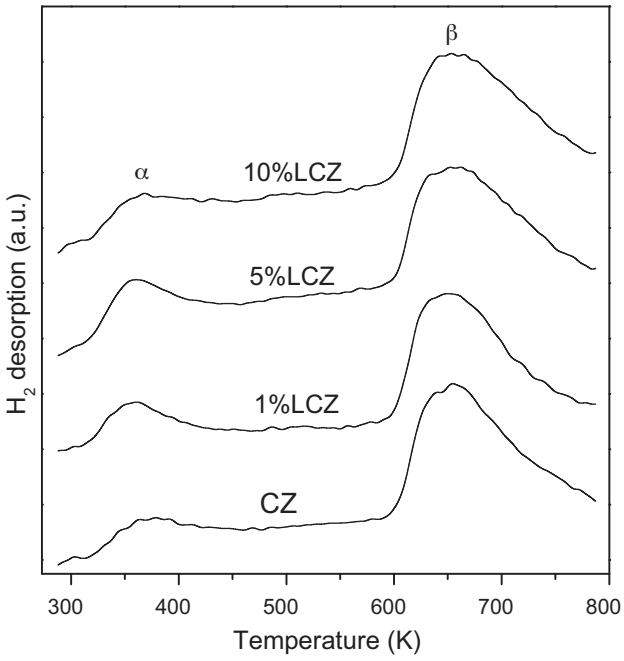

Fig. 3. H_2-TPD curves of Cu/ZrO_2 catalysts with different La loadings.

Table 4
The maximum temperature and amount of H_2 desorption over Cu/ZrO_2 catalysts with different La loadings.

Catalysts	α peak		β peak	
	T (K)	H_2 desorbed (μmol/g)	T (K)	H_2 desorbed (μmol/g)
CZ	374	13	654	63
1%LCZ	361	15	651	61
5%LCZ	360	19	656	61
10%LCZ	368	14	652	64

3.5. The basicity of La-doped Cu/ZrO_2

Fig. 4 shows the CO_2 desorption profiles obtained for Cu/ZrO_2 catalysts with different La contents. All profiles are able to be deconvoluted into three Gaussian peaks (dotted curves), which indicates that there are three types of basic sites. One desorption peak (denoted as α) appears at about 387 K, followed by another peak (denoted as β) centered at 432 K. The two peaks correspond to a weak basic site and a medium basic site, respectively. The third desorption peak (denoted as γ) located at around 530 K represents a strong basic site. Similar results with respect to the basic sites over ZrO_2 were reported by Sun and co-workers [38]. As shown in Fig. 4, the differences of the positions of these desorption peaks are small for the four studied samples, suggesting that there is no significant change of the strength of basic sites with the addition of La. However, the intensity of these desorption peaks, which is related to the number of basic sites corresponding to the CO_2 uptake, increases markedly as the La loadings increase. The number of different types of base site was evaluated by calculating the integral of each peak, and the data are summarized in Table 5. The density of total basic sites was also calculated by dividing the number of total basic sites by the BET specific surface areas (S_{BET}). It can be seen from Table 5 that both the number and the density of total basic sites enhance with the elevation of La loadings. For example, the total number and the density of basic sites on 10%LCZ were about 3 times and almost twice higher than those on sample CZ, respectively. Similar enhancement can be observed for the number of basic sites α, β and γ. Furthermore, the contributions of single basic site to the total basic sites were calculated and the results are listed in Table 5. The fractions of basic site γ to the total basic sites increased significantly with the addition of La, whereas a contrary trend was obtained for the basic site β. As for the contributions of basic site α to the total basic sites, the change was trivial with the incorporation of La, and the values kept at about 30%.

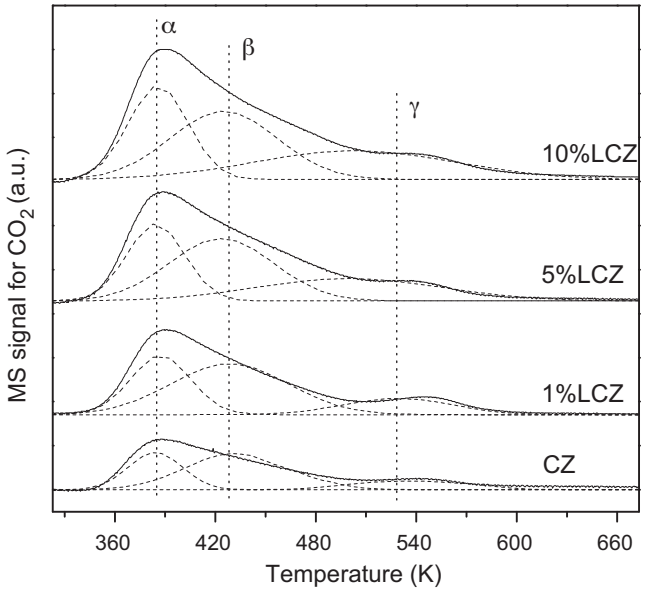

Fig. 4. CO_2-TPD curves of Cu/ZrO_2 catalysts with different La loadings.

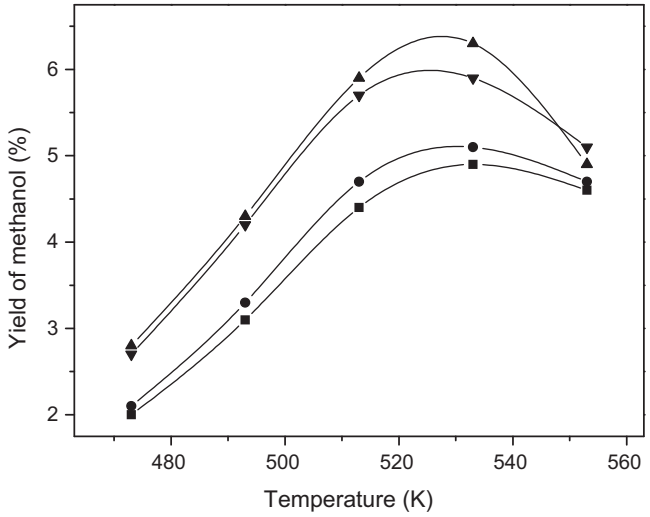

Fig. 5. Effect of reaction temperature on the yield of methanol over Cu/ZrO_2 catalysts with different La loadings. (■) CZ; (●) 1%LCZ; (▲) 5%LCZ; (▼) 10%LCZ. *Reaction conditions:* $H_2/CO_2 = 3$, $P = 3.0$ MPa, GHSV = 3600 h^{-1}.

3.6. Catalytic performance

Activity and selectivity results for the methanol synthesis from CO_2 hydrogenation over the Cu/ZrO_2 catalysts with various La loadings are summarized in Table 6. Methanol and CO are the only carbon-containing products under the present reaction conditions and traces of methane can be detected at high temperatures. As shown in Table 6, the conversion of CO_2 increases with the addition of La and a maximum of 6.2% is observed over the sample of 5%LCZ. In comparison with the La-free Cu/ZrO_2, the value increased by 17%. Further La addition leads to a decrease in CO_2 conversion. On the other hand, the selectivity for CH_3OH enhances markedly with the La dopings. The value of CH_3OH selectivity is 72.4% over 10%LCZ, which is 26% higher than that on the undoped Cu/ZrO_2. Under this reaction condition, the highest yield of CH_3OH was obtained over the 5%LCZ catalyst.

The effects of reaction temperature on the catalytic performance of Cu/ZrO_2 catalysts with different La loadings were investigated. Over the temperature range of 473–553 K, the conversion of CO_2 increased accompanied by a decrease in methanol selectivity (data not shown). This trend can be explained in terms of thermodynamics and kinetics, and the related discussion was presented in the literature [7]. The variation of methanol yield with reaction temperature is presented in Fig. 5. A maximum yield of methanol, which represents the critical point of the reaction transforming from kinetics to thermodynamics, exists for all the catalysts studied [7,39]. Furthermore, it is clear that the introduction of La is favorable for the production of methanol and the sample of 5%LCZ shows the highest methanol yield, as shown in this figure. According to the linear relationship between the natural logarithm of yield and the reciprocal of temperature that exists in the controlling region of kinetics, the values of apparent activation energy were calculated for methanol and CO production over different catalysts, and the results are listed in Table 1. It can be seen that the apparent activation energy for methanol synthesis decreases with increasing La content, whereas contrary variation trend of the apparent activation energy for CO is observed.

Table 5
The amount and distribution of basic site over Cu/ZrO_2 catalysts with different La loadings.

Catalysts	Number of total basic sites (μmol/g)	Density of total basic sites (μmol/m^2)	Number of basic sites (μmol/g) and their fraction to the number of total basic site[a] (%)		
			Site α	Site β	Site γ
CZ	19.9	0.557	5.78 (29.0)	11.0 (55.5)	3.08 (15.5)
1%LCZ	32.0	0.791	10.1 (31.6)	16.9 (52.8)	4.99 (15.6)
5%LCZ	49.9	0.924	14.7 (29.5)	21.5 (43.0)	13.7 (27.5)
10%LCZ	61.4	1.050	18.4 (30.0)	23.9 (39.0)	19.0 (31.0)

[a] The value in the parenthesis is the fraction of single basic site to the number of total basic site.

Table 6
Catalytic performance for hydrogenation of CO_2 to methanol over Cu/ZrO_2 catalysts with different La loadings.

Catalysts	CO_2 conversion (%)	CH_3OH selectivity (%)	CO selectivity (%)	CH_3OH yield (%)	TOF(Cu) $\times 10^3$ (s^{-1})	TOF(ZrO_2) $\times 10^3$ (s^{-1})
CZ	5.3	58	42	3.1	5.0	17.4
1%LCZ	5.5	60	40	3.3	4.7	11.5
3%LCZ	5.7	65	35	3.7	–	–
5%LCZ	6.2	66	34	4.3	4.5	9.6
7%LCZ	5.8	72	28	4.1	–	–
10%LCZ	5.8	72	28	4.2	5.4	7.6

Reaction conditions: $H_2/CO_2 = 3$, $T = 493$ K, $P = 3.0$ MPa, GHSV = 3600 h^{-1}.

To investigate the long-term behaviors of the studied catalysts under reaction conditions, an accelerated aging process by cycling the reactor temperature between 493 and 613 K was carried out on the undoped Cu/ZrO_2 and 5%LCZ catalysts. As shown in Fig. 6, both catalysts exhibited constant conversion values and a slight decline of methanol selectivity during the test period, indicating substantial stability of 5%LCZ and undoped Cu/ZrO_2 for CO_2 hydrogenation.

4. Discussion

4.1. The effects of La doping on the physicochemical properties

As depicted in the part of XRD investigation, the degree of crystallinity and the particle sizes of CuO and ZrO_2 on the $La–Cu/ZrO_2$ catalysts decline with increasing La loadings. It is well known that La_2O_3 is generally regarded as an additive of thermal stability and applied for various catalysts [31,40]. In our case, apart from the following calcination process, there is a transient period of high temperature during the combustion process [8]. Thus, the changes of crystal structure of CuO and ZrO_2 are connected with the thermostabilizing effect of La_2O_3. In general, two main explanations

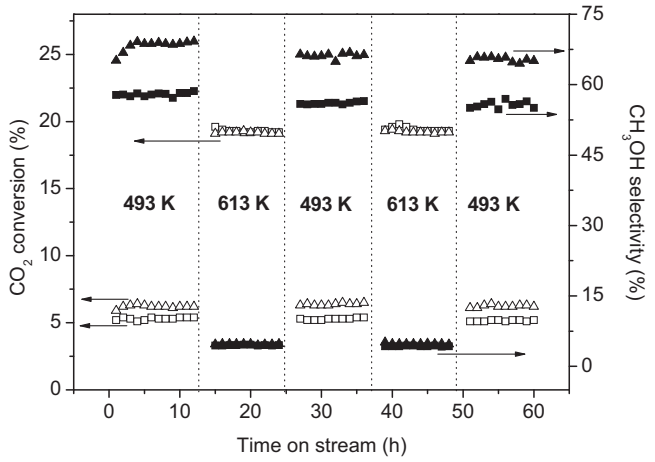

Fig. 6. Variation of CO_2 conversion and methanol selectivity with reaction time over CZ (rectangles) and 5%LCZ (triangles) catalyst. *Reaction conditions:* $H_2/CO_2 = 3$, $P = 3.0$ MPa, GHSV = 3600 h^{-1}.

are proposed for the thermostabilizing effect of La_2O_3. Firstly, during the course of heat treatment, the highly dispersed lanthanum species act as isolation island restraining the coagulation of catalyst particle and the growth of crystal grain [29,31]. Secondly, the addition of La facilitates the formation of surface defects [23], which hinders the crystallization of catalyst components and the growth of crystal grain. As stated above, the La^{3+} entered ZrO_2 phase to form $La_2Zr_2O_7$. Therefore, the crystallization and grain growth of CuO and ZrO_2 were suppressed chiefly by the defects produced during the substitution process of Zr^{4+} by La^{3+}. Correspondingly, the S_{BET} values increase from the La-free Cu/ZrO_2 to the 10%LCZ. As for S_{Cu}, the values rise first and then decrease with increasing the La loading. This is because that the effects of La doping on the S_{Cu} are double-faced. On one hand, the doping of La can enhance the dispersion of Cu. On the other hand, the position of surface Cu will be occupied partially by La, which has been demonstrated by the XPS results (Table 2). When the loading amount of La is less 5%, the former may be a predominant factor. On the contrary, the latter will prevail over the former if the loading amount is more than 5%. Therefore, the variation trend takes on a volcanic shape.

For Cu-based catalysts, the reduction characteristic is primarily related to the dispersion of Cu, though it is also affected by the interaction between CuO and support in some cases [32]. As shown in Table 3, the fractions of α peak corresponding to the fractions of highly dispersed CuO exhibit a volcano variation trend with increasing the La loading, and a maximum appears over the sample of 5%LCZ. This is in good agreement with the variation trend of the metallic copper surface area, as shown in Table 1. Avgouropoulos et al. [32,41] and Zhang et al. [33] reported that the smaller the CuO particles, the easier they are to reduce. As noted in the XRD pattern, the particle sizes of CuO decrease with the addition of La. Therefore, it is easy to understand that the position of reduction peak shifts to a lower temperature from the sample of La-free to 10%LCZ, although there is an existence of some slight discrepancy of β peak.

With the introduction of La, an expected enhancement of the amount of basic sites is obtained. The increase in S_{BET} is a direct reason for the increase in the amount of basic sites. As mentioned above, the introduction of La enhances the value of S_{BET}, which leads to an increase in the amount of exposed ZrO_2, further an increase in the exposed basic sites over ZrO_2 component. However, the increase in density of basic sites, as shown in Table 5, reveals that there are some other causes that are responsible for the

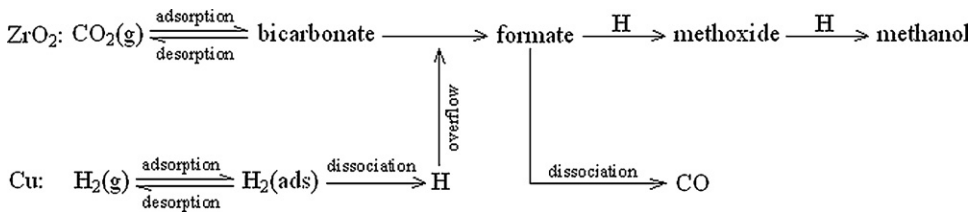

Scheme 1. The dual-site or bifunctional mechanism for methanol synthesis from CO_2 hydrogenation over Cu/ZrO_2 catalysts.

rise of the amount of basic sites, because the density of basic sites should be a constant if S_{BET} is the sole cause affecting the amount of basic sites. As well known, zirconia, a fluorite-type oxide, has face-centered-cubic (FCC) crystal structure, in which each tetravalent metal ion is surrounded by eight equivalent nearest O^{2-} ions forming the vertices of a cube. When zirconia is doped by divalent or trivalent impurity ions, a number of oxygen vacancies are created [42,43]. Wang et al. [44] reported that the existence of a high concentration of oxygen vacancies is favorable for the adsorption and activation of CO_2. Similar viewpoint was proposed by Rhodes and Bell [20], and they reported that oxygen vacancies are favorable for the adsorption and activation of CO. Obviously, in the present work, the substitution of Zr^{4+} by the La^{3+}, which leads to a marked increase in the oxygen vacancies, plays an important role for the increase in the amount of basic sites.

4.2. The effects of La doping on the catalytic properties

A number of studies have demonstrated that there are two active centers involved in the catalytic process of CO_2 hydrogenation over the Cu/ZrO_2-based catalysts [16–18,22]. One is the Cu component, and the other is the so-called "support" ZrO_2. The Cu serves to dissociatively adsorb H_2 and to provide a source of atomic hydrogen by spillover, and the ZrO_2 serves to adsorb CO_2 as bicarbonate species which then undergo stepwise hydrogenation to methanol. Fisher et al. [17] proposed that formate is a common intermediate for the synthesis of methanol and the reverse water–gas shift (RWGS) reaction. Recently, Hong et al. [45] studied the mechanism of CO_2 hydrogenation over Cu/ZrO_2 interface from first-principles kinetics Monte Carlo simulations, and their theoretical results also show that both methanol and CO are produced dominantly via the common formate intermediate. Therefore, this dual-site or bifunctional mechanism is currently accepted and it can be expressed in Scheme 1.

Obviously, based on the mechanism of CO_2 hydrogenation, the metallic copper surface area (S_{Cu}) is an important parameter for methanol synthesis. The relationship between the catalytic activity and S_{Cu} for the hydrogenation of CO_2 over Cu-based catalysts has been studied extensively. Chinchen et al. [46,47] reported that there was a linear relationship between the methanol yield of such catalysts and their copper surface areas, and similar results were also reported by other authors [14,48,49]. However, Sun et al. [39] pointed out that the methanol yield increased with the increase of S_{Cu}, but it was not a linear relationship. The same results were obtained in the recent work of Arena et al. [4]. Despite some controversies remain, there is a consensus that a large value of S_{Cu} is favorable for a high catalytic activity for the hydrogenation of CO_2. In this study, the conversion of CO_2 exhibits a volcanic variation trend with increasing the La content (Table 6), and it is consistent with the change of S_{Cu} (Table 1). This can be explained as follows. With the increase in S_{Cu}, more atomic hydrogen, which is produced by dissociative adsorption of H_2 on the surface of Cu, can be obtained. This has been confirmed by the results of H_2-TPD. Consequently, more atomic hydrogen can be supplied to the surface of ZrO_2 for the hydrogenation of the adsorbed carbon containing species. To better disclose the relation between the conversion of CO_2 and the S_{Cu}, a plot of the conversion of CO_2 versus S_{Cu} is also presented. As shown in Fig. 7, a linear relationship exists between them. As shown in Table 5, the amount of CO_2 adsorption increases continually with the increase in La loading. This trend is not consistent with the change of the conversion of CO_2, and thus it reveals that the CO_2 conversion is independent of the amount of CO_2 adsorption. These results indicate that the amount of adsorbed CO_2 is adequate, whereas the atomic hydrogen is insufficient during the hydrogenation process under the operating conditions.

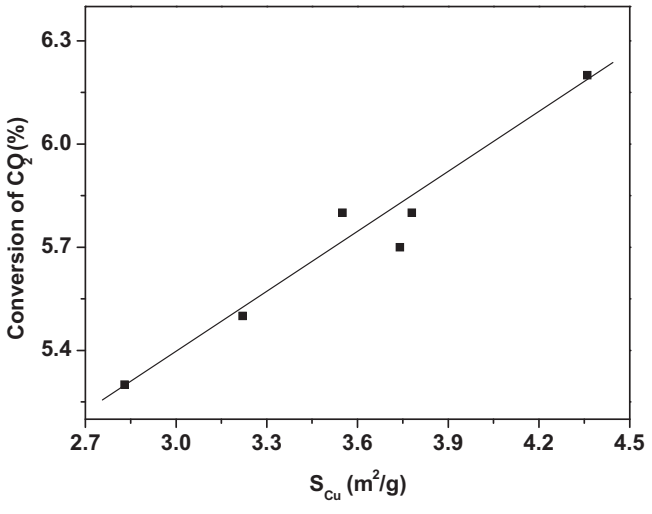

Fig. 7. The relationship between the conversion of CO_2 and the Cu surface area. *Reaction conditions:* $H_2/CO_2 = 3$, $T_R = 493$ K, $P = 3.0$ MPa, GHSV = 3600 h^{-1}.

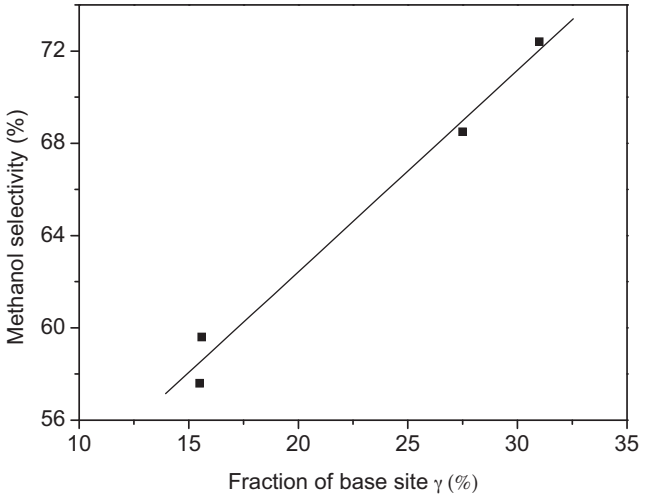

Fig. 8. The relationship between the selectivity of methanol and the fraction of γ basic site to the total amount of basic site. *Reaction conditions:* $H_2/CO_2 = 3$, $T_R = 493$ K, $P = 3.0$ MPa, GHSV = 3600 h^{-1}.

As depicted above, the selectivity of methanol over the La–Cu/ZrO_2 catalysts increases progressively with the La loadings. Although some factors affecting the methanol selectivity have been proposed, no agreement exists in the literature. For instance, Fujita et al. [50] believe that the methanol selectivity is related to the preferential emergence of smooth surface Cu sites such as Cu (1 0 0) and Cu (1 1 1). Toyir et al. [51] claimed that the high selectivity for methanol might result from the presence of Cu^+. Wang et al. [44] ascribed the enhanced selectivity for methanol to the synergistic effect between CuO and the surface oxygen vacancies of ceria. Furthermore, the effects of zirconia morphology on methanol synthesis were investigated by Rhodes and Bell [20,21]. They pointed out that the phase state of ZrO_2 influenced the methanol selectivity remarkably and higher methanol selectivity was obtained over Cu/*m*-ZrO_2 than over Cu/*t*-ZrO_2. In our case, it is found that the methanol selectivity is connected with the distribution of basic sites over the La–Cu/ZrO_2 catalysts. The results of CO_2-TPD indicate that the contributions of γ basic site to the total basic sites increase with increasing La loadings. Fig. 8 shows the relationship between the methanol selectivity and the fraction of γ basic site to the total basic sites. The methanol selectivity increases linearly with the increase in the fraction of γ basic site. This relationship can be interpreted in terms of the mechanism of CO_2 hydrogenation. As shown in Scheme 1, the formate is a common intermediate leading to both methanol and CO. It is possible that comparing with the formate adsorbed on β basic site, the formate adsorbed on γ basic site prefers to hydrogenate further to form methanol rather than dissociate to form CO. As mentioned above, with the increase in La loading, the apparent activation energy for methanol formation declined, whereas opposite trend for CO formation was observed. Evidently, the changes of apparent activation energy also support the variation of methanol selectivity with the La doping.

The turnover frequency (TOF) is an informative parameter for a heterogeneous catalytic reaction since it is an intrinsic reflection of the active site in catalysts. Conditioning on that only one active site is involved in the rate-determining step and the active sites for the title reaction are all equally active, the value of TOF should be a constant and the catalytic reaction shows a structure insensitive character [52]. As mentioned above, for the methanol synthesis via CO_2 hydrogenation over Cu/ZrO_2-based catalysts, there are two active sites (i.e. Cu and ZrO_2) participating in the catalytic reaction. Apart from the active site of ZrO_2, it is a popular viewpoint that "multisite" including Cu^0 and Cu^+ centers are involved and the stabilization of the Cu^+ ions favors the hydrogenation of CO_2 [53–55]. As far as Cu^0 center is concerned, some authors reported that the activity of Cu^0 sites is different when it locates at different positions of the crystal structure [50,54,56]. Furthermore, the rate-determining step is the hydrogenation of formate presented on the zirconia rather than the dissociative adsorption of H_2 on the surface of copper [17]. Therefore, it is easy to understand why the values of TOF found in literature, which are estimated assuming that the Cu^0 site is the sole active site and all Cu^0 site are equally active, is not a constant [4,39]. Based on these analyses, we believe that the TOF is an "apparent" TOF. Accordingly, the catalytic reaction is also an "apparent" structure sensitive reaction and similar viewpoint was proposed by Arena et al. [57]. In this study, two sets of TOF were calculated via dividing the reaction rate at 493 K by the surface area of metallic copper, as well as by the total amount of basic sites over ZrO_2, and they were denoted as TOF(Cu) and TOF(ZrO_2), respectively. As shown in Table 6, the values of TOF(Cu) decreased first and then increased with the La loadings. As to TOF(ZrO_2), a continued decline was observed. It is noteworthy that the values of TOF(Cu) are several times smaller than those of TOF(ZrO_2). On the other hand, the data of TOF(Cu) scatter in a much narrower range comparing with the distribution of TOF(ZrO_2) data. This observation indicates that a more tight correlation exists between the production of methanol and the surface area of metallic copper.

5. Conclusions

Cu/ZrO_2 catalysts with various La loadings were prepared via combustion method for methanol synthesis from CO_2 hydrogenation. The influences of La loadings on the physicochemical and catalytic properties of the La–Cu/ZrO_2 catalysts were investigated. Based on the results of this work, the following conclusions can be made:

1. With the introduction of La, Zr^{4+} is substituted partially by La^{3+} and $La_2Zr_2O_7$ is formed.
2. With the increase in La loading, the Cu surface area takes on a volcano variation trend, while the amount and density of basic site over La–Cu/ZrO_2 catalysts increase continually.
3. The conversion of CO_2 depends on the surface area of metallic Cu, and a linear relationship exists between them. The methanol selectivity increases linearly with the increase in the fraction of γ basic site to the total basic site. These results provide an evidence for the dual-site or bifunctional mechanism for methanol synthesis from CO_2 hydrogenation over Cu/ZrO_2-based catalysts.
4. A suitable amount of La is beneficial for the catalytic activity of La–Cu/ZrO_2 and a maximum methanol yield is obtained at the La loading of 5%.

Acknowledgements

The helpful suggestions provided by the anonymous reviewers are gratefully acknowledged. The authors also thank Science and Technology Commission of Shanghai Municipality (08520513600), Shanghai Municipal Education Commission (J51503) and Shanghai Institute of Technology (KJ2010-05) for financial support.

References

[1] G.A. Olah, A. Goeppert, G.K.S. Prakash, J. Org. Chem. 74 (2009) 487–498.
[2] R. Raudaskoski, E. Turpeinen, R. Lenkkeri, E. Pongrácz, R.L. Keiski, Catal. Today 144 (2009) 318–323.
[3] Y. Ma, Q. Sun, D. Wu, W.H. Fan, Y.L. Zhang, J.F. Deng, Appl. Catal. A: Gen. 171 (1998) 45–55.
[4] F. Arena, K. Barbera, G. Italiano, G. Bonura, L. Spadaro, F. Frusteri, J. Catal. 249 (2007) 185–194.
[5] X.M. Liu, G.Q. Lu, Z.F. Yan, Appl. Catal. A: Gen. 279 (2005) 241–245.
[6] R.A. Köppel, C. Stöcker, A. Baiker, J. Catal. 179 (1998) 515–527.
[7] X.M. Guo, D.S. Mao, G.Z. Lu, S. Wang, G.S. Wu, J. Catal. 271 (2010) 178–185.
[8] X.M. Guo, D.S. Mao, S. Wang, G.S. Wu, G.Z. Lu, Catal. Commun. 10 (2009) 1661–1664.
[9] J.R. Liu, J.L. Shi, D.H. He, Q.J. Zhang, X.H. Wu, Y. Liang, Q.M. Zhu, Appl. Catal. A: Gen. 218 (2001) 113–119.
[10] R. Raudaskoski, M.V. Niemelä, R.L. Keiski, Top. Catal. 45 (2007) 57–60.
[11] Y. Nitta, T. Fujimatsu, Y. Okamoto, T. Imanaka, Catal. Lett. 17 (1993) 157–165.
[12] M. Kilo, J. Weigel, A. Wokaun, R.A. Koeppel, A. Stoeckli, A. Baiker, J. Mol. Catal. A 126 (1997) 169–184.
[13] J. Słoczyński, R. Grabowski, A. Kozłowska, P. Olszewski, M. Lachowska, J. Skrzypek, J. Stoch, Appl. Catal. A: Gen. 249 (2003) 129–138.
[14] J. Słoczyński, R. Grabowski, P. Olszewski, A. Kozłowska, J. Stoch, M. Lachowska, J. Skrzypek, Appl. Catal. A: Gen. 310 (2006) 127–137.
[15] M. Lachowska, J. Skrzypek, React. Kinet. Catal. Lett. 83 (2004) 269–273.
[16] D. Bianchi, T. Chafik, M. Khalfallah, S.J. Teichner, Appl. Catal. A: Gen. 123 (1995) 89–110.
[17] I.A. Fisher, H.C. Woo, A.T. Bell, Catal. Lett. 44 (1997) 11–17.
[18] I.A. Fisher, A.T. Bell, J. Catal. 172 (1997) 222–237.
[19] I.A. Fisher, A.T. Bell, J. Catal. 178 (1998) 153–173.
[20] M.D. Rhodes, A.T. Bell, J. Catal. 233 (2005) 198–209.
[21] M.D. Rhodes, A.T. Bell, J. Catal. 233 (2005) 210–220.
[22] F. Arena, G. Italiano, K. Barbera, S. Bordiga, G. Bonura, L. Spadaro, F. Frusteri, Appl. Catal. A: Gen. 350 (2008) 16–23.
[23] Z. Ma, S.H. Overbury, S. Dai, J. Mol. Catal. A 273 (2007) 186–197.
[24] S. Sato, R. Takahashi, M. Kobune, H. Gotoh, Appl. Catal. A: Gen. 356 (2009) 57–63.
[25] Z. Boukha, L. Fitian, M. López-Haro, M. Mora, J.R. Ruiz, C. Jiménez-Sanchidrián, G. Blanco, J.J. Calvino, G.A. Cifredo, S. Trasobares, S. Bernal, J. Catal. 272 (2010) 121–130.

[26] S.R. Jain, K.C. Adiga, V.R. Pai Verneker, Combust. Flame 40 (1981) 71–79.
[27] G.C. Chinchen, C.M. Hay, H.D. Vandervell, K.C. Waugh, J. Catal. 103 (1987) 79–86.
[28] G.K. Chuah, S. Jaenicke, S.A. Cheong, K.S. Chan, Appl. Catal. A: Gen. 145 (1996) 267–284.
[29] H. Sun, Y.Q. Ding, J.Z. Duan, Q.J. Zhang, Z.Y. Wang, H. Luo, X.M. Zheng, Bioresour. Technol. 101 (2010) 953–958.
[30] L.C. Wang, Y.M. Liu, M. Chen, Y. Cao, H.Y. He, G.S. Wu, W.L. Dai, K.N. Fan, J. Catal. 246 (2007) 193–204.
[31] A. Papavasiliou, A. Tsetsekou, V. Matsouka, M. Konsolakis, I.V. Yentekakis, Appl. Catal. A: Gen. 382 (2010) 73–84.
[32] G. Avgouropoulos, T. Ioannides, H. Matralis, Appl. Catal. B: Environ. 56 (2005) 87–93.
[33] Y.P. Zhang, J.H. Fei, Y.M. Yu, X.M. Zheng, Energy Convers. Manage. 47 (2006) 3360–3367.
[34] D.L. Hoang, A. Dittmar, M. Schneider, A. Trunschke, H. Lieske, K.-W. Brzezinka, K. Witke, Thermochim. Acta 400 (2003) 153–163.
[35] N.F.P. Ribeiro, M.M.V.M. Souza, M. Schmal, J. Power Sources 179 (2008) 329–334.
[36] M.G. Lin, C. Yang, G.S. Wu, W. Wei, W.H. Li, Y.K. Shan, Y.H. Sun, M.Y. He, Chin. J. Catal. 25 (2004) 591–595.
[37] D. Bianchi, J.L. Gass, M. Khalfallah, S.J. Teichner, Appl. Catal. A: Gen. 101 (1993) 297–315.
[38] Z.Y. Ma, C. Yang, W. Wei, W.H. Li, Y.H. Sun, J. Mol. Catal. A 227 (2005) 119–124.
[39] Q. Sun, Y.L. Zhang, H.Y. Chen, J.F. Deng, D. Wu, S.Y. Chen, J. Catal. 167 (1997) 92–105.
[40] S.M. Stagg-Williams, F.B. Noronha, G. Fendley, D.E. Resasco, J. Catal. 194 (2000) 240–249.
[41] G. Avgouropoulos, T. Ioannided, Appl. Catal. A: Gen. 244 (2003) 155–167.
[42] R.X. Zhou, T.M. Yu, X.Y. Jiang, F. Chen, X.M. Zheng, Appl. Surf. Sci. 148 (1999) 263–270.
[43] T. Tabakova, V. Idakiev, J. Papavasiliou, G. Avgouropoulos, T. Ioannides, Catal. Commun. 8 (2007) 101–106.
[44] J.B. Wang, H.K. Lee, T.J. Huang, Catal. Lett. 83 (2002) 79–86.
[45] Q.J. Hong, Z.P. Liu, Surf. Sci. 604 (2010) 1869–1876.
[46] G.C. Chinchen, K.C. Waugh, D.A. Whan, Appl. Catal. 25 (1986) 101–107.
[47] G.C. Chinchen, P.J. Denny, D.G. Parker, M.S. Spencer, Appl. Catal. 30 (1987) 333–338.
[48] M. Saito, T. Fujitani, M. Takeuchi, T. Watanabe, Appl. Catal. A: Gen. 138 (1996) 311–318.
[49] R.A. Köppel, A. Baiker, Ch. Schild, A. Wokaun, Stud. Surf. Sci. Catal. 63 (1991) 59–68.
[50] S. Fujita, S. Moribe, Y. Kanamori, M. Kakudate, N. Takezawa, Appl. Catal. A: Gen. 207 (2001) 121–128.
[51] J. Toyir, P.R. de la Piscina, J.L.G. Fierro, N. Homs, Appl. Catal. B: Environ. 34 (2001) 255–266.
[52] M. Boudart, Chem. Rev. 95 (1995) 661–666.
[53] J. Toyir, P.R. de la Piscina, J.L.G. Fierro, N. Homs, Appl. Catal. B: Environ. 29 (2001) 207–215.
[54] J. Yoshihara, C.T. Campbell, J. Catal. 161 (1996) 776–782.
[55] K.P. Sun, W.W. Lu, F.Y. Qiu, S.W. Liu, X.L. Xu, Appl. Catal. A: Gen. 252 (2003) 243–249.
[56] C.V. Ovesen, B.S. Clausen, J. Schiøtz, P. Stoltze, H. Topsøe, J.K. Nørskov, J. Catal. 168 (1997) 133–142.
[57] F. Arena, G. Italiano, K. Barbera, G. Bonura, L. Spadaro, F. Frusteri, Catal. Today 143 (2009) 80–85.